

**Nontopological chiral chemical potential due to the Zeeman field in magnetic Weyl semimetals**Yi-Hang Lei,<sup>1</sup> Yong-Long Zhou,<sup>1</sup> Hou-Jian Duan,<sup>1,2</sup> Ming-Xun Deng<sup>1,2,\*</sup> Zhi-En Lu,<sup>3</sup> and Rui-Qiang Wang<sup>1,2,†</sup><sup>1</sup>Guangdong Provincial Key Laboratory of Quantum Engineering and Quantum Materials,

School of Physics and Telecommunication Engineering, South China Normal University, Guangzhou 510006, China

<sup>2</sup>Guangdong-Hong Kong Joint Laboratory of Quantum Matter, South China Normal University, Guangzhou 510006, China<sup>3</sup>Guangzhou City Construction College, Guangzhou 510925, China

(Received 28 December 2020; accepted 20 September 2021; published 27 September 2021)

As condensed-matter manifestations of the chiral anomaly, the coexistence of positive longitudinal magnetoconductivity (LMC) and the planar Hall effect (PHE) is regarded as a characteristic transport signal for the Weyl semimetal (WSM) phase. By including a finite Newtonian mass into the general linearized WSM model, we derive an analytical expression for the chiral chemical potential, which includes a topological term of the chiral anomaly and a nontopological term. The nontopological term stems from the Zeeman-field-induced tilt of the Weyl cones, which breaks the symmetry of the fermion filling between the Weyl valleys of opposite chiralities and further leads to a chiral chemical potential  $\propto \mathbf{E} \cdot \mathbf{B}$ , much as the effect of the chiral anomaly. We demonstrate that the resulting LMC is positive and can coexist with the PHE without invoking the mechanism of the chiral anomaly. Hence, the chiral chemical potential might not be exclusively respected to the chiral anomaly. Experimentally, one can distinguish the chiral anomaly from the proposed tilt mechanism by inspecting the dependence of magnetoconductivity on the Fermi energy.

DOI: [10.1103/PhysRevB.104.L121117](https://doi.org/10.1103/PhysRevB.104.L121117)

**Introduction.** Weyl semimetals (WSMs) are novel quantum states of matter, which appear as topologically nontrivial conductors where the spin-nondegenerate valence and conduction bands touch at isolated points in momentum space [1–13]. The touching points are called the Weyl nodes, as the low-energy quasiparticles near them are described by the Weyl equation [14–16]. In WSMs, the Weyl nodes always come in pairs of opposite chiralities and act as the source and sink of the Berry curvature. The projections of a pair of bulk Weyl nodes on the surface Brillouin zone are connected by topologically protected open Fermi-arc surface states. The theoretical predictions and experimental discoveries of WSMs in solid states have led to an explosion of activities in the field of condensed-matter physics [17–27].

The Berry curvature is an analog of the magnetic field but defined in reciprocal space, which has a significant impact on the dynamics of the electron wave packets [28], especially in the presence of parallel electric and magnetic fields, i.e., the  $\mathbf{E} \cdot \mathbf{B}$  term. The semiclassical description for magnetoresistance in weak magnetic fields suggests that the  $\mathbf{E} \cdot \mathbf{B}$  term leads to a positive longitudinal magnetoconductivity (LMC) and planar Hall effect (PHE) as indications of the chiral anomaly [29–34]. The chiral anomaly means the violation of the separate number conservation laws of Weyl fermions of different chiralities when  $\mathbf{E} \cdot \mathbf{B} \neq 0$ , which creates a density difference of electrons in the two opposite Weyl nodes and thus results in the so-called chiral chemical potential. Combined with the chiral magnetic effect which refers to

an electric current flowing along the direction of the applied magnetic field triggered by the chirality imbalance in the Weyl nodes, the chiral chemical potential gives rise to a current  $\propto (\mathbf{E} \cdot \mathbf{B})\mathbf{B}$ , known as the chiral-anomaly origin of the positive LMC and PHE in WSMs [34]. The chiral-anomaly-induced magnetoconductivity is quadratic in the magnetic field, i.e.,  $\Delta\sigma_{ij} \propto B_i B_j$ , which suggests the characteristic  $\cos^2\theta$  and  $\sin\theta \cos\theta$  dependences of the LMC and planar Hall conductivity, respectively, where  $\theta$  represents the angle between the electric and magnetic fields. For tilted WSMs, either the chiral anomaly or anomalous velocity, all of which depend strongly on the Berry curvature, can induce an additional linear magnetoconductivity [35–37]. In the ultraquantum limits, the positive LMC and PHE will exhibit periodic-in- $1/B$  quantum oscillations, originating from the oscillations of the nonequilibrium chiral chemical potential [38–40].

The appearance of anisotropic LMC and PHE in various systems has been attracting intense experimental and theoretical interests [29–55], but their origins are not fully distinguished and understood. The positive anisotropic LMC and PHE are widely used to identify the Weyl physics, for example, due to the emerging LMC being negative, and the anisotropic LMC and PHE measured in type-II WSMs [51–54] were demonstrated to have no relationship with the chiral anomaly, while the coexistence of positive LMC and PHE observed in the elemental semiconductor tellurium was related to Weyl physics [55]. A major issue, therefore, is whether there are alternate routes to the positive LMC and PHE in WSMs, without invoking the chiral anomaly or even the Berry curvature. This is important because the answer will directly affect the criterion for identifying a WSM by transport experiments.

\*dengmingxun@scnu.edu.cn

†wangruiqiang@m.scnu.edu.cn

In addition, the local Fermi surface is determined jointly by the particle number and the way the electrons are filled. If the filling form of the fermions is different in the two valleys, a chiral chemical potential may exist without the chiral-anomaly mechanism. How this effect manifests in the magnetotransport remains unexplored. In this Letter, by including a finite Newtonian mass into the general linearized WSM model, we derive a unified analytical expression for the LMC and planar Hall conductivity. It is found that a magnetic field will change the fermion filling by tilting the Weyl cones and then lead to a chemical potential difference  $\propto \mathbf{E} \cdot \mathbf{B}$  between the two Weyl valleys, resembling the effect of the chiral anomaly. The resulting anisotropic LMC is positive and the magnetoconductivity tensor obeys the characteristic relation, i.e.,  $\Delta\sigma_{ij} \sim B_i B_j$ , of the chiral anomaly. We also demonstrate that the positive anisotropic LMC and PHE can coexist in usual Dirac materials neither invoking the chiral anomaly nor even the Berry curvature. Hence, the coexistence of positive LMC and PHE in WSMs, or even a chiral chemical potential with  $\mathbf{E} \cdot \mathbf{B}$  dependence, might not be unique to the chiral anomaly, the observation of which could be only a necessary but not a sufficient condition for identifying the WSM phase.

*Hamiltonian and spectrum.* The low-energy fermion excitation of a magnetic WSM with two Weyl nodes subjected to a magnetic field can be characterized by an effective Hamiltonian

$$H = \chi \hbar v_F \boldsymbol{\sigma} \cdot \mathbf{k} + \lambda k^2 - g\mu_B \boldsymbol{\sigma} \cdot \mathbf{B}, \quad (1)$$

where  $\mu_B$  is the Bohr magneton,  $g$  stands for the  $g$  factor, and  $\chi = \pm 1$  denotes the chirality of the Weyl nodes. The wave vector  $\mathbf{k} = (k_x, k_y, k_z)$  is measured from the Weyl nodes  $\mathbf{K}_\chi$ ,  $v_F$  represents the Fermi velocity, and  $\boldsymbol{\sigma} = (\sigma_x, \sigma_y, \sigma_z)$  accounts for the spin Pauli matrices. The  $k$ -quadratic term with  $\hbar^2/(2\lambda)$  as the Newtonian mass describes asymmetry between the conduction and valence band, which is inevitable in real materials and has been widely adopted in Weyl and topological Dirac semimetal models [5,6,26,27]. The orbital effect of the magnetic field can be included by the Peierls substitution  $\mathbf{k} \rightarrow \mathbf{k} + \frac{e}{\hbar} \mathbf{A}$ , where  $\mathbf{A}$  is the vector potential. In the absence of asymmetry, the Zeeman effect can be gauged out and will not lead to an observable effect in the planar magnetotransport. Interestingly, as we will show, by interacting with the Newtonian mass, the Zeeman field can induce a chiral chemical potential between the Weyl valleys, akin to the effect of the chiral anomaly.

By introducing the Dirac  $\gamma$  matrices  $\gamma^0 = s_x$ ,  $\gamma^j = i s_y \sigma_j$ , and  $\gamma^5 = s_z$ , where  $s_{x,y,z}$  are Pauli matrices acting on the chirality subspace, we can represent the system in terms of the action

$$S = \int d^4x \bar{\Psi} \left[ i\gamma^\mu (D_\mu + i b_\mu \gamma^5) - \frac{\lambda g^{ij}}{\hbar v_F} D_i D_j \gamma^0 \right] \Psi, \quad (2)$$

in which  $D_\mu = \partial_\mu + ie\mathcal{A}_\mu/\hbar + iK_\mu \gamma^5$  with  $K = (0, \mathbf{K}_+)$ ,  $b = (0, g\mu_B \mathbf{B}/\hbar v_F)$ , and  $g^{\mu\nu} = \text{diag}(1, -1, -1, -1)$  is the metric tensor. Here, we have used the Einstein summation convention for simplicity, with  $i, j = 1, 2, 3$  and  $\mu, \nu = 0, \dots, 3$  as respectively the space and Minkowski space-time indices. Then, we perform a chiral gauge transformation on the Grassmann fields  $\Psi \rightarrow e^{-i\theta(x)\gamma^5} \Psi$  and  $\bar{\Psi} \rightarrow \bar{\Psi} e^{-i\theta(x)\gamma^5}$ , with

$\theta(x) = g\mu_B \mathbf{B} \cdot \mathbf{x}/\hbar v_F$ , such that the action around the gap-closing points can be given as [59]

$$S = \int d^4x \bar{\Psi} i \left( \gamma^\mu - \frac{2\lambda b_\mu}{\hbar v_F} \gamma^0 \gamma^5 \right) D_\mu \Psi. \quad (3)$$

If  $\lambda = 0$ , the Zeeman field can be fully eliminated, after which its topological effect will be transferred to the induced Chern-Simons term for the electromagnetic field [60–62]

$$S_{cs} = \frac{e^2}{16\pi^2 \hbar^2} \int d^4x \theta(x) \varepsilon^{\mu\nu\lambda\rho} F_{\mu\nu} F_{\lambda\rho}, \quad (4)$$

with  $F_{\mu\nu} = \partial_\mu \mathcal{A}_\nu - \partial_\nu \mathcal{A}_\mu$  and  $\varepsilon^{\mu\nu\lambda\rho}$  the Levi-Civita antisymmetric tensor. The variation of  $S_{cs}$  with respect to  $\mathcal{A}_\nu$  gives rise to the topological electromagnetic response  $\mathbf{j} = \frac{e^2}{2\pi^2 \hbar} \frac{g\mu_B}{\hbar v_F} \mathbf{B} \times \mathbf{E}$ , which contributes an out-of-plane magnetoconductivity. The planar magnetotransport in WSMs was demonstrated to relate closely to the chiral anomaly, which lies in the continuity equation

$$\partial_\mu j_5^\mu = -\frac{e^2}{16\pi^2 \hbar^2} \varepsilon^{\mu\nu\lambda\rho} F_{\mu\nu} F_{\lambda\rho} = \frac{e^2}{2\pi^2 \hbar^2} \mathbf{E} \cdot \mathbf{B}. \quad (5)$$

The Noether current density, according to Eq. (3), is defined as  $j_5^\mu = \bar{\Psi} (\gamma^\mu \gamma^5 - 2\lambda \gamma^0 b_\mu / \hbar v_F) \Psi$ . Within the semiclassical description, the continuity equation takes the form [31,59]  $\partial_\mu j_5^\mu = \frac{e^2}{4\pi^2 \hbar^2} \mathbf{E} \cdot \mathbf{B} \sum_\chi C_\chi^2$ , with  $C_\chi = \int \frac{d^3k}{2\pi} (\boldsymbol{\Omega}_\chi \cdot \nabla_k \epsilon_k^\chi) \frac{\partial f_k^\chi}{\partial \epsilon_k^\chi}$  the topological charge enclosed by the Fermi surface,  $f_k^\chi$  the electron distribution function, and  $\boldsymbol{\Omega}_\chi$  the Berry curvature. Recently, Rylands *et al.* demonstrated that the right-hand side of Eq. (5) can be modified by the fluctuations induced by interacting matter [62]. Here, we find the Newtonian mass term cannot enter the Chern-Simons term and thus will not alter the right-hand side of the continuity equation [59]. Therefore, the Zeeman field is trivial for the chiral anomaly, since it will not participate in particle pumping between the Weyl nodes. However, by renormalizing the current density, it can mediate the planar magnetotransport. As a consequence, for  $\lambda \neq 0$ , chiral-anomaly-independent planar magnetotransport could emerge in WSMs.

In fact, Eq. (3) gives a tilted Hamiltonian

$$\tilde{H} = s_z \hbar v_F (\boldsymbol{\sigma} + \boldsymbol{\alpha}) \cdot \mathbf{k}, \quad (6)$$

where the tilt parameter  $\boldsymbol{\alpha} = 2\lambda g\mu_B \mathbf{B}/(\hbar v_F)^2$  is modulated by the Zeeman field. Without the Zeeman field, the pristine Weyl cones are not tilted, as plotted in Fig. 1(a). As the magnetic field is turned on, the Weyl cones are shifted and tilted oppositely along the magnetic field [see Fig. 1(b)]. Even so, the local Fermi surfaces in the two fermion pockets are the same in height, since the filling form of electrons in the two fermion pockets are symmetric with each other. However, upon application of an electric field, this symmetry will be broken and the electrons in different fermion pockets can be relaxed by the intravalley impurity scattering toward different nonequilibrium Fermi surfaces, without violating the separate number conservation laws of Weyl fermions of different chiralities. As a result, a nonzero chiral chemical potential, even without the chiral anomaly, could appear between the two Weyl valleys, as illustrated by Fig. 1(d).

*Chiral chemical potential.* In the presence of the external fields, the linear-response steady-state electron distribution

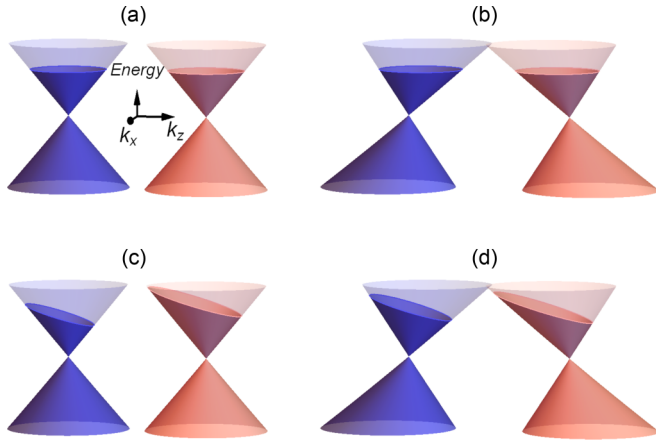


FIG. 1. Weyl cones and fermion filling in the absence (the first column) and presence (the second column) of a Zeeman field. The electron fillings of the positive and negative chiral fermion pockets are denoted by the brown and blue solid regions, with  $\mathbf{E} = \mathbf{0}$  and  $\mathbf{E} \neq \mathbf{0}$ , respectively, in the first and second row. A chiral chemical potential can be established by changing (c) the particle number via the chiral anomaly and (d) electron filling form through tilt of the Weyl cones.

function in the  $\chi$  valley takes the general form

$$f_k^\chi = f_{\text{eq}}(\epsilon_k^\chi) - f'_{\text{eq}}(\epsilon_k^\chi) g_\chi(\mathbf{k}), \quad (7)$$

where  $f_{\text{eq}}(\epsilon_k^\chi) = 1/[e^{(\epsilon_k^\chi - E_F)/(\hbar k_B T)} + 1]$  is the equilibrium distribution function,  $f'_{\text{eq}}(\epsilon_k^\chi) = \partial f_{\text{eq}}(\epsilon_k^\chi)/\partial \epsilon_k^\chi$ , and  $g_\chi(\mathbf{k})$  describes deviation of the electron distribution function from  $f_{\text{eq}}(\epsilon_k^\chi)$ . In the relaxation-time approximation,  $f_k^\chi$  follows the Boltzmann equation [38–40]

$$\mathbf{k} \cdot \nabla_{\mathbf{k}} f_k^\chi = -\frac{f_k^\chi - f_{k,\text{eq}}^\chi}{\tau_{\text{intra}}} - \frac{f_k^\chi - f_{\text{eq}}(\epsilon_k^\chi)}{\tau_{\text{inter}}}, \quad (8)$$

where  $f_{k,\text{eq}}^\chi = f_{\text{eq}}(\epsilon_k^\chi) - f'_{\text{eq}}(\epsilon_k^\chi) \langle g_\chi(\mathbf{k}) \rangle_\chi$  denotes the local equilibrium distribution function in the  $\chi$  valley, and  $\tau_{\text{intra}}$  and  $\tau_{\text{inter}}$  represent the transport relaxation times due to the electron intravalley and intervalley scattering by impurities. The average  $\langle \dots \rangle_\chi$  runs over all electron states at the Fermi level in the  $\chi$  valley, defined as

$$\langle \dots \rangle_\chi = \frac{\sum_{\mathbf{k}} \int d\epsilon [-f'_{\text{eq}}(\epsilon)] A_\chi(\epsilon, \mathbf{k}) \langle \dots \rangle}{\sum_{\mathbf{k}} \int d\epsilon [-f'_{\text{eq}}(\epsilon)] A_\chi(\epsilon, \mathbf{k})}, \quad (9)$$

where  $A_\chi(\epsilon, \mathbf{k}) = -\frac{1}{\pi} \text{Im}(\frac{1}{\epsilon + i\Gamma - \epsilon_k^\chi})$  is the spectrum function and  $\Gamma = (\tau_{\text{intra}}^{-1} + \tau_{\text{inter}}^{-1})\hbar/2$  is the impurity-induced level broadening. For a relatively weak magnetic field, the Lorentz force term  $\mathbf{k} \cdot \nabla_{\mathbf{k}} g_\chi(\mathbf{k})$  can be ignored [34–36], so we can derive for [59]

$$g_\chi(\mathbf{k}) = -e\mathbf{E} \cdot \tilde{\mathbf{v}}_k^\chi \tau_{\text{intra}} - \frac{e^2}{\hbar} (\mathbf{E} \cdot \mathbf{B}) \langle \Omega_\chi \cdot \tilde{\mathbf{v}}_k^\chi \rangle_\chi \tau_{\text{inter}}, \quad (10)$$

where  $\tilde{\mathbf{v}}_k^\chi = D_{\mathbf{k}} \nabla_{\mathbf{k}} \epsilon_k^\chi / \hbar$  and  $D_{\mathbf{k}} = (1 + e\mathbf{B} \cdot \Omega_\chi / \hbar)^{-1}$  is volume correction of the phase space due to the Berry curvature.

According to Eq. (7),  $g_\chi(\mathbf{k})$  corresponds to deviation of the local Fermi energy in the  $\chi = \pm$  valleys relative to  $E_F$ . It shows that a steady-state local Fermi surface can be formed by

cooperation of the intravalley and intervalley relaxation. Generally, the former leads to tilt of the local Fermi surfaces and the latter, related to the chiral anomaly, shifts the local Fermi surfaces toward opposite directions in energy, resulting in a chiral chemical potential between the Weyl valleys, as illustrated in Fig. 1(c). If  $\lambda = 0$ ,  $\mathbf{v}_k^\chi$  is chirality independent, which implies that the nonequilibrium Fermi surfaces in the two valleys can only be separated by the chiral anomaly. However, for  $\lambda \neq 0$ , the Zeeman field will introduce a chirality-dependent term to  $\mathbf{v}_k^\chi$  and thus can separate the nonequilibrium Fermi surfaces as well. Moreover, since the chirality-dependent term is modulated by the magnetic field, the finite  $\alpha$  resulting chiral chemical potential will be proportional to  $\mathbf{E} \cdot \mathbf{B}$ , being quite similar to the chiral anomaly.

To proceed, we assume that the Fermi level is in the vicinity of the gap-closing points and lies in the conduction band. Around the Weyl nodes, the conduction band can be characterized by  $\epsilon_k^\chi = \hbar v_F (\chi \alpha \cdot \mathbf{k} + |\mathbf{k}|)$ , in which  $\Omega_\chi = -\chi \mathbf{k} / (2|\mathbf{k}|^3)$ . As we focus on the weak magnetic field regime, i.e.,  $\ell_B \gg k_F^{-1}$  with  $k_F = E_F / \hbar v_F$  and  $\ell_B = \sqrt{\hbar / |eB|}$  the magnetic length, the volume correction of the phase space can be neglected. Then, Eq. (10) can be expressed as  $g_\chi(\mathbf{k}) = -e v_F \tau_{\text{intra}} \mathbf{E} \cdot \mathbf{k} / |\mathbf{k}| + \chi \Delta\mu$ , where, at low temperatures and in the weak impurity scattering regime, i.e.,  $f'_{\text{eq}}(\epsilon) = -\delta(\epsilon - E_F)$  and  $A_\chi(\epsilon, \mathbf{k}) = \delta(\epsilon - \epsilon_k^\chi)$ , the chiral chemical potential is given by

$$\Delta\mu = \frac{e^2 (1 - |\alpha|^2)^2 v_F \tau_{\text{inter}}}{2\hbar k_F^2} \mathbf{E} \cdot \mathbf{B} - e v_F \tau_{\text{intra}} \mathbf{E} \cdot \alpha. \quad (11)$$

A nonzero  $\Delta\mu$ , established by the chiral anomaly and tilt of the fermion pockets, is displayed respectively in Figs. 1(c) and (d). The chiral-anomaly contribution is inversely proportional to the density of states  $\propto k_F^2$ , which is in agreement with that reported in Ref. [38]. Also, we find the chiral-anomaly contribution can be suppressed by tilt of the Weyl cones. While the  $\mathbf{E} \cdot \mathbf{B}$  term is explicit in the chiral-anomaly contribution, it can be implicit in the  $\mathbf{E} \cdot \alpha$  term. Accordingly, the chiral chemical potential, even with the  $\mathbf{E} \cdot \mathbf{B}$  dependence, is only a necessary but not a sufficient condition for identifying the chiral anomaly.

*Positive anisotropic LMC and PHE.* The conductivity tensor is determined by [59]

$$\sigma_{ij} = -\frac{e^2}{\hbar} \sum_{\chi} \int \frac{d^3 \mathbf{k}}{(2\pi)^3} \varepsilon_{ijl} \Omega_\chi^l f_{\text{eq}}(\epsilon_k^\chi) - e \sum_{\chi} \int \frac{d^3 \mathbf{k}}{(2\pi)^3} \left( v_i^\chi + \frac{e B_i}{\hbar} \Omega_\chi \cdot \mathbf{v}_k^\chi \right) \frac{\partial f_k^\chi}{\partial E_j}, \quad (12)$$

where  $-\frac{\partial f_k^\chi}{\partial E_j} = f'_{\text{eq}}(\epsilon_k^\chi) \frac{\partial g_\chi(\mathbf{k})}{\partial E_j}$  and  $\Omega_\chi^i (\mathbf{v}_i^\chi)$  represents the  $i$ th component of the Berry curvature (group velocity). By fixing the electric field to be along  $\mathbf{K}_+ - \mathbf{K}_-$ , e.g., the  $z$  direction specifically, the first term corresponding to the anomalous Hall effect will not contribute to the planar magnetoelectricity and thus can be omitted. The magnetic field is assumed to lie in the  $x$ - $z$  plane, i.e.,  $\mathbf{B} = B(\cos \theta \hat{e}_z + \sin \theta \hat{e}_x)$ , where  $B$  denotes the magnitude of the magnetic field.

At low temperatures and in the weak impurity scattering regime, we can obtain a unified analytical expression for

the longitudinal and planar Hall conductivity  $\sigma_{iz} = \sigma_D \delta_{iz} + \Delta\sigma_{iz}^{\text{ch}}(B) + \Delta\sigma_{iz}^{\text{tilt}}(B)$ , where  $\sigma_D = \frac{n_e e^2}{\hbar k_F} v_F \tau_{\text{intra}}$  is the Drude conductivity, and [59]

$$\Delta\sigma_{iz}^{\text{ch}}(B) = \frac{e^2}{h} \frac{e^2 B_i B_z}{2\pi \hbar^2 k_F^2} (1 - |\alpha|^2)^2 v_F \tau_{\text{inter}}, \quad (13)$$

$$\Delta\sigma_{iz}^{\text{tilt}}(B) = \left( \frac{\Delta n_e e^2}{\hbar k_F} - \frac{e^3}{h} \frac{B_i \alpha_z + B_z \alpha_i}{\pi \hbar} \right) v_F \tau_{\text{intra}}, \quad (14)$$

are the magnetoconductivities contributed, respectively, by the chiral anomaly and tilt of the Weyl cones, with  $\Delta n_e = \tilde{n}_e - n_e \delta_{iz}$ ,  $n_e = (1/3\pi^2) k_F^3$  the carrier density,

$$\tilde{n}_e = \frac{3n_e}{2(1 - |\alpha|^2)^2} \left[ \zeta \delta_{iz} + \left( \frac{2 - 3\zeta}{|\alpha|^2} - 2 \right) \alpha_i \alpha_z \right], \quad (15)$$

and  $\zeta = \frac{1 - |\alpha|^2}{|\alpha|^2} (1 - \frac{1 - |\alpha|^2}{2|\alpha|} \ln \frac{1 + |\alpha|}{1 - |\alpha|})$ . It is evident from Eq. (13) that for  $\lambda = 0$  the chiral-anomaly contribution follows the standard relations  $\Delta\sigma_{iz}^{\text{ch}}(B) \propto B_i B_z$ , with the positive LMC  $\Delta\sigma_{zz}^{\text{ch}}(B) \propto B^2 \cos^2 \theta$  and planar Hall conductivity  $\Delta\sigma_{xz}^{\text{ch}}(B) \propto B^2 \sin \theta \cos \theta$ . While for a finite  $\lambda$ , the chiral-anomaly contribution will be slightly suppressed and since  $\alpha$  also contains  $B$ , the  $B$  dependence of  $\Delta\sigma_{iz}^{\text{ch}}(B)$  becomes more complicated. The second term of Eq. (14) is attributable to the anomalous velocity determined by the Berry curvature, which is relevant to the chiral magnetic effect. If  $\lambda = 0$ ,  $\Delta n_e = 0$ , and then  $\Delta\sigma_{iz}^{\text{tilt}}(B)$  vanishes. If  $\lambda \neq 0$ , the joint effect of the nontopological chiral chemical potential  $\propto \mathbf{E} \cdot \alpha$  and the anomalous velocity  $\frac{eB_i}{\hbar} (\mathbf{\Omega}_\chi \cdot \mathbf{v}_k^x)$ , will induce a magnetoconductivity proportional to the magnetic field and the tilt parameter, which is consistent with the results reported in Refs. [35–37]. Here, the tilt parameter is modulated by the magnetic field, and therefore, the anomalous-velocity contribution is also  $B$ -quadratic. Besides, for a finite  $\lambda$ , the carrier density will be renormalized by the magnetic field, which also enhances the nontopological magnetoconductivity. The first term of Eq. (15) is angular independent, such that the angular dependence of the nontopological contribution should be  $\sim B_i B_z$ . To better understand this contribution, we approximate  $\Delta n_e$  to leading order in the magnetic field and arrive at

$$\Delta n_e = \frac{|\alpha|^2}{5\pi^2} \left( 2\delta_{iz} - \frac{\alpha_i \alpha_z}{|\alpha|^2} \right) k_F^3. \quad (16)$$

Now, it is clear that the first term of Eq. (14) would contribute a positive LMC  $\propto \lambda^2 B^2 (2 - \cos^2 \theta)$  and planar Hall conductivity  $\propto -\lambda^2 B^2 \sin \theta \cos \theta$ , both proportional to  $k_F^2$ , in sharp contrast to the  $1/k_F^2$  dependence of the chiral-anomaly contribution, as plotted in Figs. 2(a)–2(d). By adjusting the Fermi energy, when  $E_F$  exceeds a critical value, e.g.,  $E_c$  in Figs. 2(e) and 2(f),  $\Delta\sigma_{iz}^{\text{tilt}}(B)$  dominates over  $\Delta\sigma_{iz}^{\text{ch}}(B)$  and a  $\pi/2$ -phase shift will occur in oscillation of the positive LMC, and meanwhile, the planar Hall current will reverse its direction. These behaviors can act as signatures to experimentally distinguish the tilt mechanism from the chiral anomaly.

**Conclusion and remarks.** In summary, we have demonstrated that a nontopological chiral chemical potential can appear in WSMs, without involving the mechanism of the chiral anomaly. The cooperation between the nontopological chiral chemical potential and the chiral-magnetic-effect

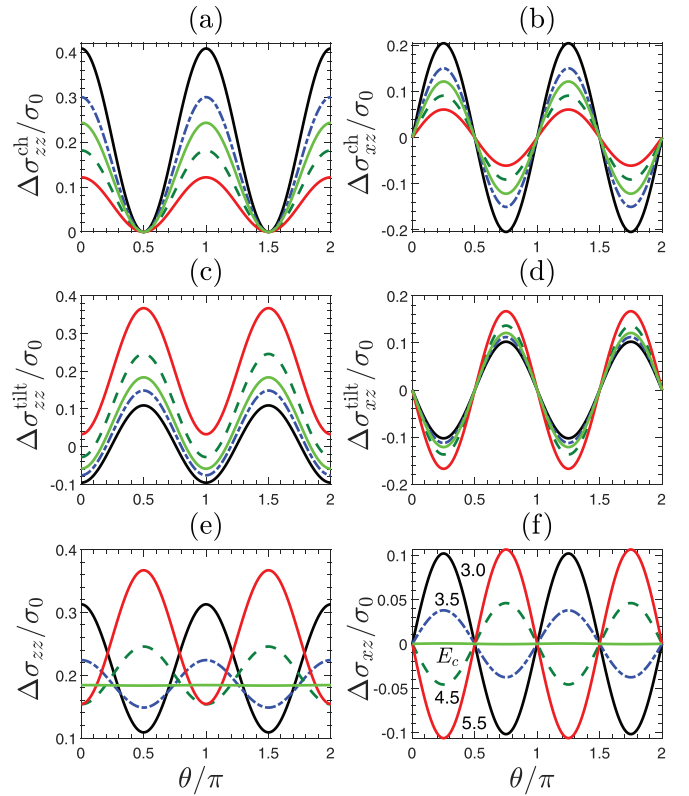


FIG. 2. LMC (left panels) and planar Hall conductivity (right panels) as functions of  $\theta$  for  $|\alpha| = \lambda \ell_z / (\hbar v_F \ell_B^2) = 0.1$ , i.e.,  $\lambda/\hbar v_F = 0.05\ell_0$ ,  $\ell_B = 0.8\ell_0$ , and  $\ell_z \equiv 2g\mu_B/(\hbar v_F) = 1.3\ell_0$ , with  $\tau_{\text{inter}}/\tau_{\text{intra}} = 5$  and  $E_F = (3.0, 3.5, 4.5, 5.5)\hbar\omega_c$ , where  $\omega_c = v_F/\ell_B$  denotes the cyclotron frequency and  $E_c = 3.89\hbar\omega_c$  for the present parameters. Here, for convenience, we chose  $\sigma_0 = \sigma_D|_{k_F \rightarrow 1/\ell_0}$  and  $\ell_0 = \sqrt{\frac{\hbar}{e|B=1\text{ T}|}} \sim 25\text{ nm}$ , respectively, as the unit of conductivity and length. The parameters are accessible in real materials, such as in the Weyl material  $\text{Cd}_3\text{As}_2$ , with  $\lambda = 11.5\text{ eV \AA}^2$ ,  $\hbar v_F = 0.889\text{ eV \AA}$  [56], and the  $g$  factor is able to reach a value about 50 [57]. The ratio  $\tau_{\text{inter}}/\tau_{\text{intra}} \sim e^2 k_0^2 d_0^2/2$  is determined jointly by the properties of the WSMs and impurities [58], where  $d_0$  is the characteristic length of scatterers and  $k_0$  denotes the separation of the two Weyl nodes.

related anomalous velocity can introduce an additional magnetoconductivity. On the other hand, the nontopological local chemical potential can result in an anisotropic LMC and PHE very similar to the ones originating from the chiral anomaly. Therefore, the chiral chemical potential, as well as the coexistence of the positive LMC and PHE, is not unique to the topological properties of WSMs, the observation of which cannot be exclusive evidence for the chiral anomaly. The proposed tilt mechanism and the chiral anomaly are two independent mechanisms to cause the positive LMC and PHE, and so chiral-anomaly-like magnetoconductivity can exist even in systems without the chiral anomaly. In Ref. [59], we consider the cases both for the bulk and surface states of 3D topological insulators [63], where the chiral anomaly is shown to be turned off, but the positive LMC and PHE due to the Zeeman field still remain, whose forms are similar to that in WSMs. Our findings suggest that, to identify WSMs by magnetotransport experiments, further experimental work is



needed to diagnose the chiral anomaly from other nontopological mechanisms.

*Acknowledgments.* This work was supported by the National NSF of China under Grants No. 11904107, No. 11874016, No. 12174121, and No. 12104167, the Guang-

dong NSF of China under Grant No. 2020A1515011566, GDUPS(2017), the Science and Technology Program of Guangzhou under Grant No. 2019050001, and the Guangdong provincial universities innovation project (2019GK-TSCX164).

- 
- [1] X. Wan, A. M. Turner, A. Vishwanath, and S. Y. Savrasov, *Phys. Rev. B* **83**, 205101 (2011).
  - [2] K.-Y. Yang, Y.-M. Lu, and Y. Ran, *Phys. Rev. B* **84**, 075129 (2011).
  - [3] G. Xu, H. Weng, Z. Wang, X. Dai, and Z. Fang, *Phys. Rev. Lett.* **107**, 186806 (2011).
  - [4] S. M. Young, S. Zaheer, J. C. Y. Teo, C. L. Kane, E. J. Mele, and A. M. Rappe, *Phys. Rev. Lett.* **108**, 140405 (2012).
  - [5] Z. Wang, Y. Sun, X.-Q. Chen, C. Franchini, G. Xu, H. Weng, X. Dai, and Z. Fang, *Phys. Rev. B* **85**, 195320 (2012).
  - [6] Z. Wang, H. Weng, Q. Wu, X. Dai, and Z. Fang, *Phys. Rev. B* **88**, 125427 (2013).
  - [7] Z. K. Liu, B. Zhou, Y. Zhang, Z. J. Wang, H. M. Weng, D. Prabhakaran, S.-K. Mo, Z. X. Shen, Z. Fang, X. Dai, Z. Hussain, and Y. L. Chen, *Science* **343**, 864 (2014).
  - [8] M. Neupane, S.-Y. Xu, R. Sankar, N. Alidoust, G. Bian, C. Liu, I. Belopolski, T.-R. Chang, H.-T. Jeng, H. Lin, A. Bansil, F. Chou, and M. Z. Hasan, *Nat. Commun.* **5**, 3786 (2014).
  - [9] S.-Y. Xu, I. Belopolski, N. Alidoust, M. Neupane, G. Bian, C. Zhang, R. Sankar, G. Chang, Z. Yuan, C.-C. Lee, S.-M. Huang, H. Zheng, J. Ma, D. S. Sanchez, B. Wang, A. Bansil, F. Chou, P. P. Shibayev, H. Lin, S. Jia *et al.*, *Science* **349**, 613 (2015).
  - [10] B. Q. Lv, N. Xu, H. M. Weng, J. Z. Ma, P. Richard, X. C. Huang, L. X. Zhao, G. F. Chen, C. E. Matt, F. Bisti, V. N. Strocov, J. Mesot, Z. Fang, X. Dai, T. Qian, M. Shi, and H. Ding, *Nat. Phys.* **11**, 724 (2015).
  - [11] B. Q. Lv, H. M. Weng, B. B. Fu, X. P. Wang, H. Miao, J. Ma, P. Richard, X. C. Huang, L. X. Zhao, G. F. Chen, Z. Fang, X. Dai, T. Qian, and H. Ding, *Phys. Rev. X* **5**, 031013 (2015).
  - [12] L. Lu, Z. Wang, D. Ye, L. Ran, L. Fu, J. D. Joannopoulos, and M. Soljačić, *Science* **349**, 622 (2015).
  - [13] N. P. Armitage, E. J. Mele, and A. Vishwanath, *Rev. Mod. Phys.* **90**, 015001 (2018).
  - [14] H. Nielsen and M. Ninomiya, *Phys. Lett. B* **130**, 389 (1983).
  - [15] M. E. Peskin and D. V. Schroeder, *An Introduction to Quantum Field Theory* (Westview Press, Boulder, CO, 1995).
  - [16] G. E. Volovik, *The Universe in a Helium Droplet* (Oxford University Press, Oxford, UK, 2003).
  - [17] D.-W. Zhang, S.-L. Zhu, and Z. D. Wang, *Phys. Rev. A* **92**, 013632 (2015).
  - [18] M.-X. Deng, W. Luo, R.-Q. Wang, L. Sheng, and D. Y. Xing, *Phys. Rev. B* **96**, 155141 (2017).
  - [19] D.-W. Zhang, Y.-Q. Zhu, Y. X. Zhao, H. Yan, and S.-L. Zhu, *Adv. Phys.* **67**, 253 (2018).
  - [20] X.-S. Li, C. Wang, M.-X. Deng, H.-J. Duan, P.-H. Fu, R.-Q. Wang, L. Sheng, and D. Y. Xing, *Phys. Rev. Lett.* **123**, 206601 (2019).
  - [21] M.-X. Deng, Y.-Y. Yang, W. Luo, R. Ma, C.-Y. Zhu, R.-Q. Wang, L. Sheng, and D. Y. Xing, *Phys. Rev. B* **100**, 235105 (2019).
  - [22] M. Yang, Q.-T. Hou, and R.-Q. Wang, *New J. Phys.* **21**, 113057 (2019).
  - [23] M. Yang, Q.-T. Hou, and R.-Q. Wang, *New J. Phys.* **22**, 033015 (2020).
  - [24] Y.-Y. Yang, M.-X. Deng, H.-J. Duan, W. Luo, and R.-Q. Wang, *Phys. Rev. B* **101**, 205137 (2020).
  - [25] C. M. Wang, H.-Z. Lu, and S.-Q. Shen, *Phys. Rev. Lett.* **117**, 077201 (2016).
  - [26] C. M. Wang, H.-P. Sun, H.-Z. Lu, and X. C. Xie, *Phys. Rev. Lett.* **119**, 136806 (2017).
  - [27] H. Li, H. Liu, H. Jiang, and X. C. Xie, *Phys. Rev. Lett.* **125**, 036602 (2020).
  - [28] D. Xiao, M.-C. Chang, and Q. Niu, *Rev. Mod. Phys.* **82**, 1959 (2010).
  - [29] A. A. Burkov, *Phys. Rev. Lett.* **113**, 247203 (2014).
  - [30] A. A. Burkov, *Phys. Rev. B* **91**, 245157 (2015).
  - [31] D. T. Son and B. Z. Spivak, *Phys. Rev. B* **88**, 104412 (2013).
  - [32] V. A. Zyuzin, *Phys. Rev. B* **95**, 245128 (2017).
  - [33] K.-S. Kim, H.-J. Kim, and M. Sasaki, *Phys. Rev. B* **89**, 195137 (2014).
  - [34] S. Nandy, G. Sharma, A. Taraphder, and S. Tewari, *Phys. Rev. Lett.* **119**, 176804 (2017).
  - [35] D. Ma, H. Jiang, H. Liu, and X. C. Xie, *Phys. Rev. B* **99**, 115121 (2019).
  - [36] K. Das and A. Agarwal, *Phys. Rev. B* **99**, 085405 (2019).
  - [37] S. Ghosh, D. Sinha, S. Nandy, and A. Taraphder, *Phys. Rev. B* **102**, 121105(R) (2020).
  - [38] M.-X. Deng, G. Y. Qi, R. Ma, R. Shen, R.-Q. Wang, L. Sheng, and D. Y. Xing, *Phys. Rev. Lett.* **122**, 036601 (2019).
  - [39] M.-X. Deng, H.-J. Duan, W. Luo, W. Y. Deng, R.-Q. Wang, and L. Sheng, *Phys. Rev. B* **99**, 165146 (2019).
  - [40] M.-X. Deng, J.-Y. Ba, R. Ma, W. Luo, R.-Q. Wang, L. Sheng, and D. Y. Xing, *Phys. Rev. Research* **2**, 033346 (2020).
  - [41] J. Xiong, S. K. Kushwaha, T. Liang, J. W. Krizan, M. Hirschberger, W. Wang, R. J. Cava, and N. P. Ong, *Science* **350**, 413 (2015).
  - [42] C.-Z. Li, L.-X. Wang, H. Liu, J. Wang, Z.-M. Liao, and D.-P. Yu, *Nat. Commun.* **6**, 10137 (2015).
  - [43] Y. Wang, E. Liu, H. Liu, Y. Pan, L. Zhang, J. Zeng, Y. Fu, M. Wang, K. Xu, Z. Huang, Z. Wang, H.-Z. Lu, D. Xing, B. Wang, X. Wan, and F. Miao, *Nat. Commun.* **7**, 13142 (2016).
  - [44] Y.-Y. Lv, X. Li, B.-B. Zhang, W. Y. Deng, S.-H. Yao, Y. B. Chen, J. Zhou, S.-T. Zhang, M.-H. Lu, L. Zhang, M. Tian, L. Sheng, and Y.-F. Chen, *Phys. Rev. Lett.* **118**, 096603 (2017).
  - [45] X. Huang, L. Zhao, Y. Long, P. Wang, D. Chen, Z. Yang, H. Liang, M. Xue, H. Weng, Z. Fang, X. Dai, and G. Chen, *Phys. Rev. X* **5**, 031023 (2015).
  - [46] H. Li, H. He, H.-Z. Lu, H. Zhang, H. Liu, R. Ma, Z. Fan, S.-Q. Shen, and J. Wang, *Nat. Commun.* **7**, 10301 (2016).

- [47] C.-L. Zhang, S.-Y. Xu, I. Belopolski, Z. Yuan, Z. Lin, B. Tong, G. Bian, N. Alidoust, C.-C. Lee, S.-M. Huang, T.-R. Chang, G. Chang, C.-H. Hsu, H.-T. Jeng, M. Neupane, D. S. Sanchez, H. Zheng, J. Wang, H. Lin, C. Zhang *et al.*, *Nat. Commun.* **7**, 10735 (2016).
- [48] Y. Zhao, H. Liu, J. Yan, W. An, J. Liu, X. Zhang, H. Wang, Y. Liu, H. Jiang, Q. Li, Y. Wang, X.-Z. Li, D. Mandrus, X. C. Xie, M. Pan, and J. Wang, *Phys. Rev. B* **92**, 041104(R) (2015).
- [49] A. A. Taskin, H. F. Legg, F. Yang, S. Sasaki, Y. Kanai, K. Matsumoto, A. Rosch, and Y. Ando, *Nat. Commun.* **8**, 1340 (2017).
- [50] S.-H. Zheng, H.-J. Duan, J.-K. Wang, J.-Y. Li, M.-X. Deng, and R.-Q. Wang, *Phys. Rev. B* **101**, 041408(R) (2020).
- [51] J. Meng, H. Xue, M. Liu, W. Jiang, Z. Zhang, J. Ling, L. He, R. Dou, C. Xiong, and J. Nie, *J. Phys.: Condens. Matter* **32**, 015702 (2019).
- [52] D. D. Liang, Y. J. Wang, W. L. Zhen, J. Yang, S. R. Weng, X. Yan, Y. Y. Han, W. Tong, W. K. Zhu, L. Pi, and C. J. Zhang, *AIP Adv.* **9**, 055015 (2019).
- [53] Q. Liu, F. Fei, B. Chen, X. Bo, B. Wei, S. Zhang, M. Zhang, F. Xie, M. Naveed, X. Wan, F. Song, and B. Wang, *Phys. Rev. B* **99**, 155119 (2019).
- [54] J. Yang, W. L. Zhen, D. D. Liang, Y. J. Wang, X. Yan, S. R. Weng, J. R. Wang, W. Tong, L. Pi, W. K. Zhu, and C. J. Zhang, *Phys. Rev. Materials* **3**, 014201 (2019).
- [55] N. Zhang, G. Zhao, L. Li, P. Wang, L. Xie, B. Cheng, H. Li, Z. Lin, C. Xi, J. Ke, M. Yang, J. He, Z. Sun, Z. Wang, Z. Zhang, and C. Zeng, *Proc. Natl. Acad. Sci. USA* **117**, 11337 (2020).
- [56] A. Chen, D. I. Pikulin, and M. Franz, *Phys. Rev. B* **95**, 174505 (2017).
- [57] J. Feng, Y. Pang, D. Wu, Z. Wang, H. Weng, J. Li, X. Dai, Z. Fang, Y. Shi, and L. Lu, *Phys. Rev. B* **92**, 081306(R) (2015).
- [58] X. Huang, H. Geng, and L. Sheng, *Phys. Rev. B* **103**, 115208 (2021).
- [59] See Supplemental Material at <http://link.aps.org/supplemental/10.1103/PhysRevB.104.L121117> for detailed derivations of the chiral anomaly, local nonequilibrium Fermi surface, and the transport coefficients, as well as discussions about the positive LMC and PHE in the bulk and surface states of 3D topological insulators.
- [60] K. Fujikawa, *Phys. Rev. D* **21**, 2848 (1980).
- [61] A. A. Zyuzin and A. A. Burkov, *Phys. Rev. B* **86**, 115133 (2012).
- [62] C. Rylands, A. Parhizkar, A. A. Burkov, and V. Galitski, *Phys. Rev. Lett.* **126**, 185303 (2021).
- [63] X.-L. Qi and S.-C. Zhang, *Rev. Mod. Phys.* **83**, 1057 (2011).